Developmental Biology 369 (2012) 191–198

Contents lists available at SciVerse ScienceDirect

Developmental Biology

journal homepage: www.elsevier.com/locate/developmentalbiology

Abnormal vasculature interferes with optic fissure closure in *lmo2* mutant zebrafish embryos

Omri Weiss [1], Rivka Kaufman [1], Natali Michaeli, Adi Inbal *

Department of Medical Neurobiology, Institute for Medical Research Israel–Canada, The Hebrew University-Hadassah Medical School, Jerusalem, Israel

ARTICLE INFO

Article history:
Received 27 March 2012
Received in revised form
16 June 2012
Accepted 19 June 2012
Available online 20 July 2012

Keywords:
Zebrafish
Optic fissure
Coloboma
Ocular vasculature
lmo2

ABSTRACT

Ocular coloboma is a potentially blinding congenital eye malformation caused by failure of optic fissure closure during early embryogenesis. The optic fissure is a ventral groove that forms during optic cup morphogenesis, and through which hyaloid artery and vein enter and leave the developing eye, respectively. After hyaloid artery and vein formation, the optic fissure closes around them. The mechanisms underlying optic fissure closure are poorly understood, and whether and how this process is influenced by hyaloid vessel development is unknown. Here we show that a loss-of-function mutation in *lmo2*, a gene specifically required for hematopoiesis and vascular development, results in failure of optic fissure closure in zebrafish. Analysis of ocular blood vessels in *lmo2* mutants reveals that some vessels are severely dilated, including the hyaloid vein. Remarkably, reducing vessel size leads to rescue of optic fissure phenotype. Our results reveal a new mechanism leading to coloboma, whereby malformed blood vessels interfere with eye morphogenesis.

Introduction

During early stages of eye formation, invagination of the optic vesicle results in generation of a bilayered optic cup with a groove along its ventral margin. This groove, named optic fissure (also known as choroidal fissure or embryonic fissure), provides an opening through which the hyaloid artery enters and the hyaloid vein leaves the developing eye. Subsequently, the margins of the optic cup close around these vessels. In human embryos the optic fissure closes during the 6–7th weeks of gestation (Barishak, 2001) and in zebrafish embryos the fissure is closed by 2 days post-fertilization (dpf). Failure of optic fissure closure leaves a gap named ocular coloboma, which can lead to impaired vision and even blindness (Chang et al., 2006).

Many genetic perturbations result in failure of optic fissure closure and, as a result, coloboma (Chang et al., 2006; Gregory-Evans et al., 2004). Studies in model organisms, primarily mouse and zebrafish, suggest that such genetic lesions can lead to abnormal dorsoventral patterning of the optic vesicle, reduced expression of ventral eye or periocular mesenchyme genes, excessive cell proliferation and tissue fusion defects (Kim et al., 2007; Lupo et al., 2011; McLaughlin et al., 2007; Mui et al., 2005). Hence, multiple mechanisms are involved in optic fissure closure underscoring the complexity of this process. However, a mechanistic understanding of the process of optic fissure closure is still missing, and hence it is poorly understood why this process sometimes fails.

In this work we show that ocular blood vessel development is an important factor that can affect optic fissure closure. Specifically, we identify zebrafish *lmo2* mutants that fail to close the optic fissure at 2 dpf. Investigation of vasculature in these mutants demonstrates that some ocular vessels, including vessels located in the optic fissure, are grossly dilated and integrity of the vessels appears to be compromised. The increased vessel size is flow-dependent and underlies the failure of optic fissure closure, thus identifying a new mechanism leading to coloboma. Together, our results suggest new roles for Lmo2 in vascular development and demonstrate how abnormal vascular development interferes with organ morphogenesis.

Materials and methods

Fish lines and genotyping

lmo2^{vu270} heterozygous carriers were maintained in AB background. Identification of carriers was performed either by crosses and observation of mutant phenotype in ~25% of progeny or using the following dCAPS (Neff et al., 2002) genotyping protocol: a 211 bp fragment from *lmo2* locus was PCR-amplified from genomic DNA using forward primer 5' GACTGTTTGGTCAGGACGGACTCTA 3' and reverse primer 5' CCGTTGAGTTTGGTCCACTC 3'. PCR product was digested with HindIII and run on 3% agarose gel. Whereas wild-type allele remains uncut, mutant allele is digested

* Corresponding author. Fax: +972 2 6439736.
E-mail address: adi.inbal@ekmd.huji.ac.il (A. Inbal).
[1] These authors contributed equally to this work.

0012-1606/$ - see front matter © 2012 Elsevier Inc. All rights reserved.
http://dx.doi.org/10.1016/j.ydbio.2012.06.029

to 186 bp and 25 bp fragments. *Tg*(*rx*3:*Gal*4-*VP*16)*vu*271: medaka *rx*3 4 kb promoter region (Rembold et al., 2006) was cloned into EcoRV site in pTolDest (Villefranc et al., 2007) to generate *rx*3-destination plasmid. *Gal*4-*VP*16 coding sequence was inserted downstream of *rx*3 promoter by Gateway LR recombination reaction with pME-*Gal*4*VP*16 (Kwan et al., 2007) to generate *rx*3:*Gal*4-*VP*16 plasmid. *Tg*(*rx*3:*Gal*4-*VP*16) fish were generated by co-injection of *rx*3:*Gal*4-*VP*16 DNA and Tol2 transposase synthetic RNA as described (Kawakami et al., 2004). Additional lines used in this work: *Tg*(*UAS*:*GFP*)*vu*157 (Inbal et al., 2006); *Tg*(*kdrl*:*egfp*)*s*843 (Jin et al., 2005); *Tg*(*kdrl*:*HsHRAS-mCherry*)*s*896 (Chi et al., 2008).

Expression constructs, RNA synthesis and morpholino injection

pCS2-*lmo*2: total RNA was isolated from 1 dpf wild-type embryos with TriFast (Peqlab), and *lmo*2 coding sequence was amplified by RT-PCR (SuperScript, Invitrogen) and cloned into pCS2+ vector between XbaI and EcoRI sites. pCS2-*lmo*2-C94X: C94X mutation was introduced by site directed mutagenesis in pCS2-*lmo*2. Sequence was confirmed for both constructs and synthetic capped RNA was prepared by NotI digestion and transcription with SP6 polymerase (mMESSAGE mMACHINE, Ambion). MO1-*tnnt2a* (Sehnert et al., 2002) has been described.

Tissue sectioning and staining

Embryos were fixed in 4% paraformaldehyde overnight at 4 °C, washed with PBT, dehydrated in EtOH series and embedded in JB4 resin (Polysciences, Inc.) according to manufacturer's instructions. 4 µm sections were cut with LKB 8800 Ultratome III microtome and stained with methylene blue—azure II (Humphrey and Pittman, 1974).

In situ hybridization, antibody labeling and TUNEL

Whole-mount in situ hybridization (ISH) using riboprobes was performed according to standard protocols. BMPurple (Roche) was used as blue substrate. For double labeling by ISH and immunohistochemistry, first ISH was carried out using Fast Red (Roche) as red fluorescent substrate. Subsequently, embryos were washed with PBT (PBS+0.1% Tween-20) followed by two 5 min washes with PBSTX (PBS+0.1% Tween-20+0.1% Triton X-100) and blocked for 2 h at room temperature in 500 µl blocking buffer (PBSTX+10% BSA+1% donkey serum). Incubation with primary antibody was done overnight at 4 °C in 500 µl blocking buffer. Embryos were then washed at least 6 times with PBSTX for 30 min and incubated with secondary antibody overnight at 4 °C in 500 µl incubation buffer (PBSTX+1% BSA+0.1% donkey serum). Following six 15 min washes with PBT, embryos were washed with PBS, mounted in glycerol or agarose and imaged. Primary antibodies used in this work were rabbit anti-GFP at 1:500 (Torrey Pines Biolabs) and rabbit anti-phospho-Histone H3 at 1:750 (Santa Cruz). Secondary antibody was Alexa Fluor 488 donkey anti-rabbit at 1:400 (Jackson ImmunoResearch).

For TUNEL (terminal deoxynucleotidyl transferase dUTP nick end labeling), embryos were fixed overnight with 4% paraformaldehyde at 4 °C, washed with PBT, gradually transferred to MeOH and kept at −20 °C. Subsequently, embryos were rehydrated with PBT, permeabilized by incubation in 0.1% Na–Citrate and 10 µg/ml proteinase K in PBT, washed with PBT and TUNEL reaction was performed using in situ cell death detection kit, TMR red (Roche) according to manufacturer's instructions.

Microangiography and imaging

For microangiography embryos were anesthetized and injected with 2–3 nl of 2 mg/ml fluorescein isothiocyanate dextran molecular weight 2,000,000 (Sigma). Dextran was injected into the sinus venosus and embryos were imaged within 30 min. To block pigmentation when imaging embryos older than 24 hours post-fertilization (hpf), embryos were raised in the presence of 0.003% *N*-Phenylthiourea (PTU) (Sigma) from 22 hpf. Images were acquired using Zeiss LSM 700 confocal microscope and Discovery.V8 stereomicroscope with Axiocam MRc digital camera (Zeiss).

Data quantification and statistical analysis

Quantification of proliferating and apoptotic cells was performed by manually counting labeled cells from single confocal sections covering the entire depth of the eye. Counted cells were marked to avoid re-counting of the same cell. Cell counts were performed independently by two researchers, and results were highly similar.

We used χ^2 statistics to test for goodness of fit (rescue experiments) and Student's *t*-test (proliferation and cell death experiments).

Results

lmo2 mutant zebrafish

To identify new mechanisms underlying failure in optic fissure closure we searched for mutations causing ocular coloboma utilizing an F3 ENU-mutagenesis genetic screen. We identified a mutant line designated *vu*270 in which failure of optic fissure closure was evident at 2 dpf (Fig. 1A and B). Two other phenotypes observed in the mutants were enlarged, inflated-looking

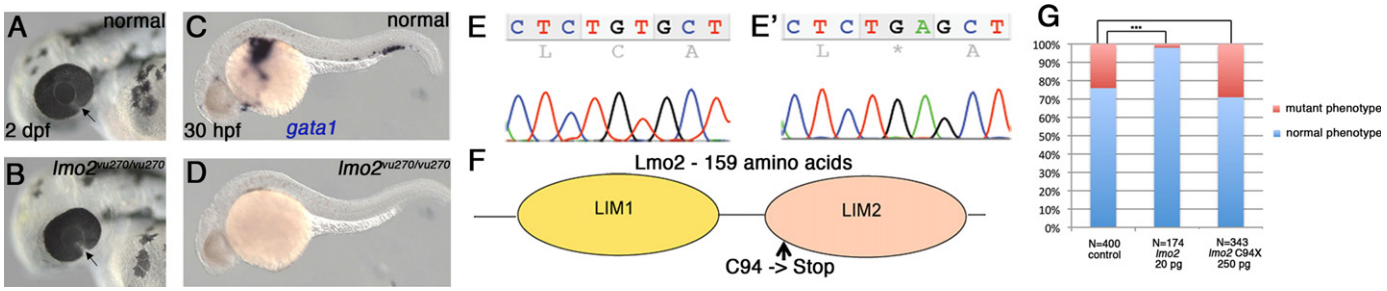

Fig. 1. *lmo*2 mutant zebrafish embryos. (A and B) Heads of normal (A) and *lmo*2 mutant (B) live embryos at 2 dpf. Arrows point at the optic fissure. (C and D) 30 h post-fertilization (hpf) normal (C) and *lmo*2 mutant (D) embryos labeled for RBC marker *gata1*. (E and E') Chromatograms showing normal *lmo*2 (E) and mutant *lmo*2^{vu270} (E') coding sequence at the mutation site. (F) Schematic presentation of Lmo2 protein and the site of predicted truncation in Lmo2 encoded by *vu*270 allele (arrow). (G) Quantification of rescue of *lmo*2 mutant phenotypes by injection of RNA encoding normal Lmo2 or Lmo2^{C94X}. Numbers are summary of at least two independent experiments. (***$p < 0.0001$).